NEUTRON-DEFICIENT DECAYS IN THE ^{48}Ni REGION WITH ACTAR TPC*

A. Ortega Moral

on behalf of the E791 Experiment Collaboration†

LP2iB, Gradignan, France

Received 29 November 2022, accepted 6 February 2023, published online 22 March 2023

Since the first indirect measurements of the two-proton radioactivity in 2002, some theoretical descriptions have been able to reproduce experimental results until the 2-proton radioactivity was established for ^{67}Kr at RIKEN, with a lifetime about 20 times lower than predicted. New theory inputs have recently been developed, predicting angular distributions of the emitted protons for some of the two-proton emitters that need to be confirmed experimentally. An experiment at GANIL/LISE3 facility was performed in May 2021 aiming to produce one of the 2-proton emitters (^{48}Ni) and to measure the angular distribution of the emitted protons. We used the ACTAR TPC detector to implant the ions and perform the tracking of their proton decays. In addition, other exotic nuclei in the ^{48}Ni region were produced. For several of them we have found a first evidence of exotic decays such as β-delayed 3- and 2-proton emission or low-energy proton branches for β-delayed single-proton emission.

DOI:10.5506/APhysPolBSupp.16.4-A16

1. Introduction

In this work, we study nuclei in the neutron-deficient region around $Z = 28$, $N = 20$. The main decay modes are β^+ emission or electron capture, followed by single- or multiple-proton emission from the daughter(s), (β-delayed proton emission). In the case of ^{48}Ni and ^{45}Fe which are nuclei beyond the proton drip line, this decay mode is in competition with the direct two-proton emission. We analyse these decays for the most exotic bound nuclei in the region from $Z = 24, N = 19$ to $Z = 28, N = 21$: ^{48,49}Ni, ^{45,46,47}Fe, ^{46}Mn, ^{45}Fe, ^{43}Cr, and ^{40}V.

* Presented at the Zakopane Conference on Nuclear Physics, *Extremes of the Nuclear Landscape*, Zakopane, Poland, 28 August–4 September, 2022.

† The list of E791 Experiment Collaboration members can be found at the end of the article.

2. Exotic decays

2.1. Two-proton radioactivity

The two-proton radioactivity occurs when the nucleus is beyond the proton drip line and the number of protons is even. Due to the pairing effect, there is an extra binding energy for the two protons to either stay together inside the nucleus or be emitted, while the single-proton emission is energetically forbidden.

The two-proton radioactivity was already predicted in the 1960s by Goldanski [1], and since the first indirect measurements in 2002 [2], theoretical predictions started to appear to explain this decay mode. The most relevant models were the 3-body model by Grigorenko *et al.* [3] and the shell model corrected half-lives (Brown *et al.*) or "hybrid model" [4].

The calculated half-lives for ^{45}Fe, ^{54}Zn, and ^{48}Ni as well as the angular distribution already measured for ^{45}Fe were in agreement with the experimental results. Then the half-life of ^{67}Kr was found to be 20 times lower than theoretically predicted [5].

At that moment and more recently, two new different models appeared to explain this inconsistency: Semi-analytical R-matrix calculation, Grigorenko *et al.* [6] and Gamow Coupled Channels Wang and Nazarewicz [7]. Since the proton angular distributions are at the moment only measured for ^{45}Fe [8], further experiments for the proton emitters (^{48}Ni, ^{67}Kr, and ^{54}Zn) are required to disentangle the nature of the inconsistencies, in the first place between theory and experiments, and secondly, between the different predicted angular distributions. Dedicated TPC detectors are needed for that.

2.2. β-delayed proton emission

The β-delayed proton(s) emission is a typical decay mode in the neutron-deficient nuclei that are far from stability. It is an emission of proton(s) from the daughter(s) of the nuclei after the β^+ or electron capture decay of the parent. If the proton is emitted from an excited state, valuable information about the energies can be extracted, generally not accessible through other means. Measurements made with a TPC detector present certain advantages to classical silicon detector experiments such as transparency to β particles, meaning no background at low energies. Also, when a multiple-proton emission occurs, a further study can be done concerning the angles between the emitted protons, the measurement of their individual energies, and the information about the branching ratio of the different β–p(s) emissions.

3. The experiment

The experiment was performed at GANIL, France (May 2021) aiming to produce ^{48}Ni and the neighbouring nuclei. The beam was produced by fragmentation of a 74.5A MeV ^{58}Ni beam of 5 μA on a 210 μm thick $^{\mathrm{nat}}$Ni target. The exotic fragments were then selected using the LISE3 spectrometer [9] and finally implanted in the ACTive TARget Time Projection Chamber [10–12] gas device filled with Ar(90%) + iC$_4$H$_{10}$(10%) at 300 mbar to study their decays. Other silicon and position detectors were placed along the beam line to identify the different isotopes of the cocktail beam.

ACTAR TPC is a gaseous detector whose development was strongly motivated by the measurement of the two-proton radioactivity. The nucleus of interest enters the chamber and stops in the gas. The implantation is followed by the decay (proton emission) of the nucleus.

The charged particle(s) ionize the gas along their trajectories. The electrons drift under the influence of a homogeneous, vertical electric field towards the detection plane (128 × 128 independent pads) where the signal is amplified and collected. The signal on each pad is sampled in 256 time cells for a third dimension reconstruction. This results in a 4 mega-voxel discretized volume which allows for a full 3D reconstruction of the tracks, as illustrated in Fig. 1.

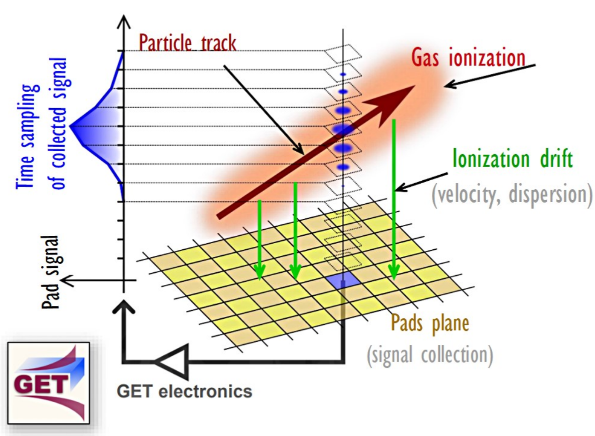

Fig. 1. Particle interaction inside ACTAR. The process of gas ionization, drifting of the electrons towards the pixel plane, and signal collection (amplitude and time). The signal is collected on the 2D pad plane and sampled in time for a 3D signal reconstruction of the track.

4. Analysis

The first step of the analysis concerns the identification of the implanted nuclei: this is commonly made with a 2D identification matrix (time of flight (ToF) of the isotope *versus* the energy deposit in a silicon detector). In the present work, due to the large momentum acceptance of the spectrometer in the experiment, a 4-dimensional identification analysis is performed to better separate the isotopes that overlap in ToF. This is done considering also the information given by other detectors located in the beam line. This identification process is still not optimized and thus the present results are preliminary.

The implantation and the decay come as different events in the acquisition due to the lifetime of the nuclei. After the identification, we search within a time window (about 10 half-lives) for decay events fulfilling some spatial condition (< 10 mm) between the stopping point of the implantation and the starting point of the decay in the detection plane. Each decay is then classified by the number of emitted particles using an adaptation of the Hough 3D algorithm [13]. The number of tracks in the event and a pre-calculation of the extreme points of the track(s) are given as a starting point to perform a 3D Bragg peak fit of the proton(s) track(s).

5. Preliminary results

5.1. Two-proton emission

For ^{48}Ni, we identified a total of eight events. Half of them decayed by two-proton emission and the others by β-delayed proton emission. In Fig. 2, an example of several sequential events is shown. The angles between the protons, resulting from the tracks fit, are shown in Fig. 3 together with

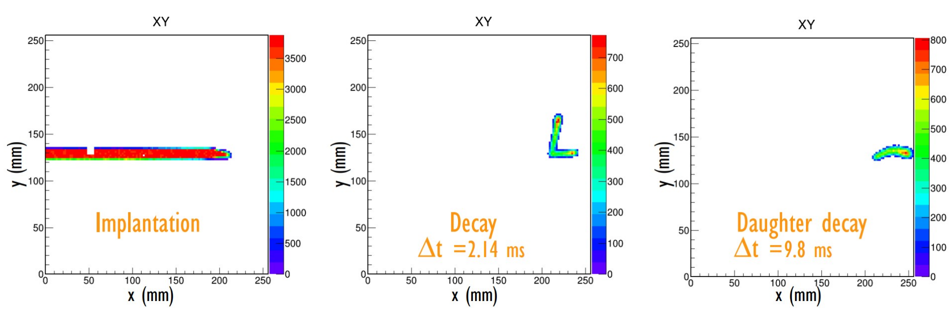

Fig. 2. Sequence of events measured in ACTAR TPC. First, the ^{48}Ni enters the detector and stops correctly inside the detection volume (left). Some time after, the 2-proton decay of ^{48}Ni is observed from the same point as the stopping of the implantation (center). Finally, the daughter (^{46}Fe) β–p decay is observed since this nucleus is still unstable.

previous results measured by Pomorski *et al.* [14]. Although the statistics is limited, no angles greater than 90° between the two protons were observed neither from the events from previous experiments nor from the present one.

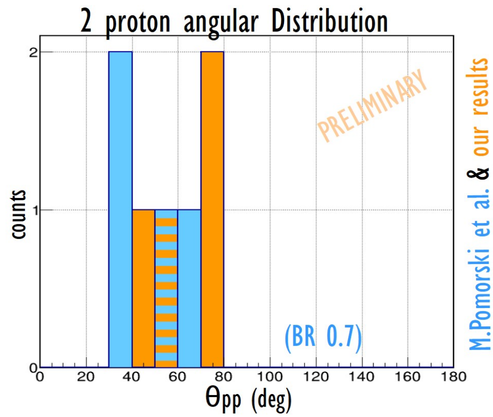

Fig. 3. Two-proton angular distribution for ^{48}Ni.

In the case of ^{45}Fe, we got a total of 26 ions implanted in the detector. Thirteen of them decayed by two-proton emission and the rest by β-delayed one-proton emission. The measured relative angles between the 2 protons are statistically in agreement with the previous results [13] in Fig. 4.

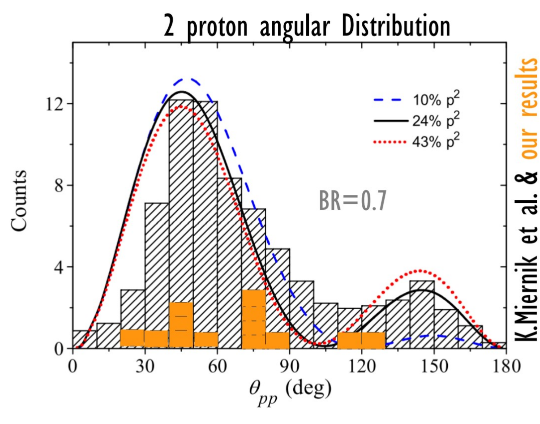

Fig. 4. Two-proton angular distribution for ^{45}Fe.

5.2. β-delayed proton emission

The first evidence and direct observation of β-delayed 3-proton emission is found for ^{49}Ni. For this nucleus with a total of 57 events correctly implanted, a preliminary estimate of the branching ratio for the decay modes is measured: β–1p ($67^{+7}_{-7}\%$), β–2p ($31^{+7}_{-7}\%$) and β–3p ($2^{+4}_{-1}\%$). The estimation of the error is calculated considering binomial distributions for each of the different decay modes with respect to the total number of measured events. Also, β-delayed two-proton emission is found for the first time for ^{46}Mn, ^{47}Fe and ^{40}Ti. Moreover, new β-delayed low-energy proton emission for ^{46}Mn and ^{40}Ti with astrophysical interest were observed as well.

6. Next steps

After the optimization of the identification process, the proton energy distribution can be measured for each of the β-delayed proton emitters. The branching ratio of their different decay modes can be obtained as well. Using this information, previous results measured with silicon detectors [1] can be completed at low energies. For the most exotic nuclei, an attempt will be made to identify the transitions and reconstruct their partial decay schemes. A second experiment for the ^{67}Kr two-proton emitter at RIKEN is also planned to measure the angular distribution and confirm or disprove the most recent theoretical inputs of the two-proton radioactivity.

REFERENCES

[1] V. Goldansky, *Nucl. Phys.* **19**, 482 (1960).
[2] C. Dossat *et al.*, *Phys. Rev. C* **72**, 054315 (2005).
[3] L.V. Grigorenko *et al.*, *Phys. Rev. C* **64**, 054002 (2001).
[4] B.A. Brown, F.C. Barker, *Phys. Rev. C* **67**, 041304(R) (2003).
[5] T. Goigoux *et al.*, *Phys. Rev. Lett.* **117**, 162501 (2016).
[6] L.V. Grigorenko *et al.*, *Phys. Rev. C* **95**, 021601 (2017).
[7] S.M. Wang, W. Nazarewicz, *Phys. Rev. Lett.* **120**, 212502 (2018).
[8] K. Miernik *et al.*, *Phys. Rev. Lett.* **99**, 192501 (2007).
[9] R. Anne *et al.*, *Nucl. Phys. A* **575**, 125 (1994).
[10] T. Roger *et al.*, *Nucl. Instrum. Methods Phys. Res. A* **895**, 126 (2018).
[11] J. Giovinazzo *et al.*, *Nucl. Instrum. Methods Phys. Res. A* **892**, 114 (2018).
[12] B. Mauss *et al.*, *Nucl. Instrum. Methods Phys. Res. A* **940**, 498 (2019).
[13] C. Dalitz *et al.*, *Image Processing On Line* **7**, 184 (2017).
[14] M. Pomorski *et al.*, *Phys. Rev. C* **83**, 061303 (2011).

The list of E791 Experiment Collaboration members:

P. Acher, B. Blank, C. Borcea, L. Cáceres, M. Caamaño, F. Cresto, F. De Oliveira, A. De Roubin, B. Fernández, D. Fernández, J. Lois Fuentes, M. Gerbaux, J. Giovinazzo, S. Grevy, M. Hukkaneng, A. Husson, O. Kamalou, T. Kurtukian-Nieto, J. Michaud, J. Pancin, J. Piot, M. Pomorski, D. Regueira, T. Roger, A.M. Sánchez Benitez, O. Sorlin, M. Stanoiu, C. Stodel, J.-C. Thomas, M. Vanderbrouck.